High-throughput experimental evolution using barcoded strains of *Saccharomyces cerevisiae*

Vincent J. Fasanello*, Carlos A. Botero†, Ping Liu*, Justin C. Fay‡

* Division of Biology and Biomedical Sciences; Washington University School of Medicine in St. Louis; St. Louis, Missouri; 63110

† Department of Biology; Washington University in St. Louis; St. Louis, Missouri; 63130

‡ University of Rochester; Rochester, New York; 14627

Running Title: Barcoded Experimental Evolution

Keywords: Experimental Evolution, *Saccharomyces cerevisiae*, Genetic Barcode, Fitness Assay

Corresponding Author: Vincent Fasanello, Washington University in St. Louis, Campus Box 1137, One Brookings Drive, St Louis, MO 63130-4899

ABSTRACT

Experimental evolution of microbes can be used to empirically address a wide range of questions about evolution. Because fitness assays are a central component of experimental evolution, they can limit the scope and throughput of such studies. We created an experimental evolution system in *Saccharomyces cerevisiae* that utilizes genetic barcoding to overcome this challenge. We confirm that barcode insertions do not alter fitness and can be used to detect fitness differences of 2%. Using this system, we examine here the effects of ploidy, stress, and population bottleneck size on the evolutionary dynamics and fitness gains in a total of 76 experimentally evolving populations by conducting 2,136 fitness assays and analyzing 532 longitudinal-evolutionary samples collected from evolving populations. Our experimental treatments generated distinct fitness effects and evolutionary dynamics quantified via multiplexed fitness assays and barcode lineage tracking, respectively, demonstrating the utility of this new resource for designing and improving high-throughput studies of experimental evolution. The approach described here provides a framework for future studies using this experimental system.

INTRODUCTION

Experimental evolution in microorganisms such as yeast, bacteria, and viruses has been used to answer evolutionary questions that are experimentally intractable in organisms with longer generation times (de Varigny 1892; Garland and Rose 2009; Kassen 2014; Van den Bergh et al.

2018). A central benefit of most experimental evolution systems is the ability to replicate and repeat evolution as well as the ability to store and compete evolved, intermediate, and ancestral strains (Van den Bergh et al. 2018). Indeed, if there is a single unifying theme to what we have learned from experimental evolution it is that adaptation is universal and often repeatable due to parallel changes down to the molecular level (Burke, Liti, and Long 2014; Kohn and Anderson 2014; Bailey et al. 2017; Graves et al. 2017; Bailey, Guo, and Bataillon 2018). The power of this approach has led to numerous investigations of the effects of population size (Schoustra et al. 2009; A. C. Gerstein et al. 2011; Bailey et al. 2017) and structure (Bell and Gonzalez 2011; Kryazhimskiy, Rice, and Desai 2012; Low-Décarie et al. 2015), mutation rate (Lenski, Sniegowski, and Gerrish 1997; Loewe, Textor, and Scherer 2003; Perfeito et al. 2007; Swings et al. 2017), and various environmental treatments (B. S. Hughes, Cullum, and Bennett 2007; R. Dhar et al. 2011; Riddhiman Dhar et al. 2013; Zhou et al. 2013; Horinouchi et al. 2015; Huang et al. 2018).

Measuring adaptation by changes in fitness is a core requirement of experimental evolution that often limits its implementation. Fitness assays involve direct competition of individuals or populations against one another or a common reference, and traditionally have been calculated using neutral markers scored by plating assays. For example, the long-term experimental evolution conducted by Lenski and colleagues is scored by counting colonies that can ferment arabinose based on colony color (Lenski et al. 1991). Many recent studies use fluorescently marked strains such that co-cultured strains can be counted by flow-cytometry (Gresham et al. 2008; A. C. Gerstein et al. 2011; Selmecki et al. 2015). However, the number of fitness assays,

and thereby the resolution of those assays remain limited, which poses a challenge for large-scale projects. The primary constraint limiting the scale of these studies is that measuring fitness requires replicate assays, often under a variety of conditions. For example, an experiment with 100 strains evolved in a single environment would require 600 fitness assays if one were to measure, in triplicate, the fitness of each ancestral strain and each evolved strain in relation to a common reference. Additionally, each of these assays would require measuring the frequency of the two strains at the beginning and end of the competition. Equally important is the ability to detect small changes in fitness, which is directly related to the number of replicate assays per strain and the noise of the assay itself.

Genetic barcodes can vastly increase the throughput of these analyses through pooled-fitness assay designs. In a barcoding approach, each strain is marked by insertion of a unique neutral DNA sequence into its genome (i.e., its barcode), enabling the easy quantification of the relative abundance of multiple strains when they are simultaneously competed against a common reference. Microarrays (Roth et al. 2009) and more recently, direct sequencing of barcodes (Giaever and Nislow 2014), have been used to measure the effects of thousands of single gene deletions using this approach. Barcodes have also been used in experimental evolution. A pool of half a million barcoded yeast strains made it possible to detect and track the fate of each barcoded lineage (Blundell and Levy 2014; Levy et al. 2015). Other research with these barcoded strains has focused on isolating strains with adaptive mutations, tracking lineages during evolution and quantifying fitness via competition-based fitness assays (Venkataram et al. 2016; Li et al. 2018).

In this study we describe a novel set of barcoded yeast strains and characterize their utility for experimental evolution. The system is composed of a collection of *Saccharomyces cerevisiae* strains, individually barcoded with unique 20 bp sequences inserted upstream of the *HO* locus; this barcoding strategy offers a number of advantages for experimental evolution. First, cross-contamination between populations with different barcodes can be detected and monitored. Second, populations can be initiated with mixtures of multiple barcodes for tracking adaptive dynamics (Kao and Sherlock 2008; Selmecki et al. 2015). Finally, fitness can be measured from the entire set of strains in a single pooled fitness assay, which dramatically increases efficiency relative to earlier methods. To demonstrate the capabilities of this system we began by conducting a series of proof-of-concept fitness assays and subsequently applied what we learned in a short, 25-day (~250-generation) experimental evolution. These analyses confirm that barcode insertions (1) do not alter the fitness of our source strains, (2) enable the detection of fitness differences as small as 2%, and (3) provide a means of measuring fitness differences and evolutionary dynamics for individual lineages from pooled samples obtained at different stages of experimental evolution. We highlight the advantages of multiplexing samples with indexing and the importance of limiting molecular contamination between initial sampling and library construction. Taken together, this system represents a new resource for designing and improving high-throughput studies in experimental evolution.

MATERIALS AND METHODS

Strains, media and culture methods

Barcoded yeast strains were constructed using two haploid derivatives of a diploid strain collected from an Oak tree in Pennsylvania (YPS163) (Sniegowski, Dombrowski, and Fingerman 2002): YJF153 (MATa, *HO*::dsdAMX4) and YJF154 (MATalpha, *HO*::dsdAMX4). Barcoded kanMX deletion cassettes were amplified from the MoBY plasmid collection (Magtanong et al. 2009) with primers containing homology to the promoter region (-1,129 to -1,959) of *HO*. A set of 92 barcoded cassettes were selected based on confirmation of correct barcodes by sequencing (Table S1), then transformed into YJF153 and confirmed by PCR. Barcoded diploid strains were made by mating barcoded haploids (YJF153) to YJF154, and confirming diploids by mating-type PCR (Huxley, Green, and Dunbam 1990). Strains were stored at -80°C as 15% glycerol stocks.

All evolution and fitness assays were conducted in complete minimal medium (CM;2% dextrose, 0.17% yeast nitrogen base without amino acid and ammonium sulfate, 0.5% ammonium sulfate, 0.13% dropout mix complete without yeast nitrogen base) with or without additional stresses in 96-deep well plates (2.2-ml poly-propylene plates, square well, v-conical bottom; Abgene AB-0932) covered with rayon acrylate breathable membranes (Thermo Scientific, 1256705). Growth plates were incubated at 30°C for 24 hours inside an incubator (VWR, Forced Air Incubator, basic, 120v, 7 cu. ft.) with agitation using a horizontal electromagnetic microplate shaker (Union Scientific LLC, 9779-TC). Saturated 24-hour culture was diluted (1:1000) into fresh medium at the same time each day to initialize the next round of growth for all evolution and fitness assays.

Starting material for all evolution and fitness assays originated from -80°C freezer stocks of the barcoded yeast strains. Yeast were revived from -80°C freezer stocks via a single round of growth (1 day, 10 generations) under standard culture conditions for these assays. Samples collected during our experiments were stored as both (1) 15% glycerol stocks at -80°C to maintain viable freezer stocks of yeast populations, and (2) pelleted samples at -20°C for DNA extraction.

Experimental design

Proof-of-concept fitness assays: The design of this new system for experimental evolution began with a proof-of-concept analysis in which (1) methods were optimized, and (2) it was confirmed that the fitness of multiple strains in pooled samples could be simultaneously and accurately measured by sequencing-based competition assay methods. This initial step involved measuring the fitness of 91 barcoded yeast strains relative to an ancestral reference strain simultaneously using a sequencing-based fitness assay (Figure 1, A.). Ten replicate fitness assays were conducted under standard culture conditions. Briefly, 92 yeast strains were revived from -80°C freezer stocks, mixed in equal proportions (i.e., such that each strain comprised 1/92 of the pooled population), and diluted (1:1000) into fresh medium to initialize the two-day proof-of-concept fitness assays. Samples were obtained from the undiluted initial mixtures and, 20 generations later, from the final overnight population cultures. Fitness was measured by the change in barcode abundance relative to a 'reference' strain (d1H10) from 10 replicates over the two-day period of approximately 20 generations, for a total of 920 fitness assays (92 barcodes x 10 replicates). See "Fitness Calculations", below for a full description of the

145 competition-based fitness assay methodology and for calculations of fitness from barcode
146 abundance data. DNA was isolated separately for each sample using a ZR Fungal/Bacterial DNA
147 Kit (Zymo Research D6005) in individual 2.0 mL screw-cap tubes following the manufacturer's
148 instructions. Physical cell disruption by bead-beating was carried out in a mixer mill (Retsch,
149 MM 300) at 30 Hz (1800 min^{-1}) for ten minutes (1-minute on, 1-minute off, times ten cycles).
150 Following extraction, DNA was amplified with forward/reverse primers containing a 9-12 bp
151 index for multiplex sequencing. PCR products were quantified, pooled and purified to form a
152 single multiplexed library for sequencing. Additional control samples were also included in the
153 library to track barcode cross-contamination. See "Library Construction and Sequencing",
154 below, for a detailed description of the library preparation protocol used for these and all other
155 samples.
156
157 **250-Generation evolution experiment**: After establishment of the feasibility of the analysis
158 strategy and optimization of the culture, assay, and processing methods, yeast strains were
159 evolved for 25 days (i.e., ca. 250 generations at 9.97 generations per day) under different
160 scenarios of selection in a second set of experiments. Specifically, 152 yeast strains were
161 evolved by serial dilution in one of six different treatments (Figure 1, B1.; See Table S2 for
162 treatment descriptions). Evolutionary treatments involved growth in either complete media
163 (CM), CM with ethanol (8% by volume) or CM with NaCl (0.342 M). Serial transfers were
164 achieved either through standard dilution (1:1000), reduced dilution (1:250), or increased
165 dilution (1:4000). Haploid and diploid yeast were evolved under standard conditions to assess
166 the effects of ploidy. To initialize the evolution experiment, barcoded yeast strains were revived

from -80°C freezer stocks. Barcoded yeast pairs slated to evolve in sympatry were then mixed in equal proportions and diluted in fresh medium, according to the experimental design, to begin the 250 generations of evolution.

Samples were obtained from the initial undiluted mixtures and on day 25 (ca. 250 generations later), from the final overnight population cultures to serve as the starting material for the Generation-0 fitness assays and Generation-250 fitness assays, respectively (See: *End-point assay of relative fitness change*). Additional Samples were obtained at generations 0, 100, 150, 200, 220, 240, and 250 for evolutionary dynamics analysis (See: *Evolutionary Dynamics*). Two assays, evolutionary dynamics and end-point relative fitness, were developed to characterize the evolutionary processes and fitness change outcomes observed in the 250-generation evolution experiment:

Evolutionary Dynamics: Relative proportions of pairs of barcoded yeast strains evolved in sympatry were quantified at generations 0, 100, 150, 200, 220, 240, and 250 from a total of 532 evolutionary dynamics samples collected from the evolving populations. Briefly, evolutionary dynamics samples were pooled for DNA extraction such that there was no barcode overlap within pools. DNA was subsequently extracted (see the “Proof-of-concept fitness assays” section, above, for details). Libraries were constructed for sequencing as described in the “Library construction and sequencing” section, below. From these evolutionary dynamics data, the time-point (t-max) and magnitude (m-max) of the maximum change in relative abundance in comparison to the starting conditions, the time-point (t-max-rate) and magnitude (m-max-

189 rate) of the maximum rate of change between adjacent time-points, the time-point (t-max-diff)
190 max difference (m-max-diff) in BC proportions, and the total cumulative change in sympatric
191 barcode relative abundance across all time-points were quantified. Barcodes approaching
192 fixation (hereafter referred to as “fixed barcodes”) were also noted and were defined as cases
193 in which a single barcode from the sympatric barcode pair obtained (and maintained) a
194 proportion of 0.95 or greater by (through) generation 250 of the evolution experiment.
195
196 *End-point assays of relative fitness:* The second assay type, the “end-point assay of relative
197 fitness”, was designed to assess the fitness of a given focal strain relative to a reference via
198 barcoded competition-based fitness assay; these measures, if taken at the start and end of an
199 experimental evolution, provide a means of measuring fitness change. In this case, the assay
200 involved quantifying barcode fitness using pooled samples from generation 0 (Figure 1, B2.)
201 and generation 250 (Figure 1, B3.) from the 250-generation evolution experiment (Figure 1,
202 B1.). Briefly, Generation-0 and Generation-250 yeast strains were revived and samples from
203 each time point were pooled such that there was no overlap in barcoded yeast strain identity
204 within each pool. Pools of revived generation-0 and generation-250 yeast were independently
205 combined in equal proportion (50 pooled-yeast : 50 ancestral reference) with an ancestral
206 reference strain (re: an ‘unevolved’ barcoded yeast strain); these pooled samples were then
207 diluted into fresh medium to initialize the fitness assays. Four replicate Fitness assays were
208 conducted for each pool of generation-0 and generation-250 yeast. Fitness assays employed a
209 standard 1:1000 transfer dilution across all samples. Samples evolved in CM plus additional
210 stresses were assayed in the same media type that they were evolved in. Diploid yeast were

competed against a diploid reference strain (strain ID: d1H10), while haploid yeast were competed against the haploid version of this same reference (strain ID: h1H10). In these assays, yeast samples for DNA extraction were obtained from the undiluted initial mixtures (fitness assay starting material), and, 20 generations later, from the final overnight population cultures (fitness assay end) to assess fitness of generation-0 and generation-250 yeast strains. See "Fitness Calculations", below, for a full description of fitness assay methodology and for calculations of fitness from fitness assay barcode abundance data. Libraries were constructed for sequencing as described in the "Library construction and sequencing section", below.

Library construction and sequencing: Barcode sequencing libraries for the proof-of-concept fitness assays and all samples from both components of the 250-generation evolution experiment were constructed by amplification of the MoBY barcodes (Magtanong et al. 2009) with primers containing Ion Torrent adaptors with indexes to distinguish samples from one another (Table S3).

PCR products for library construction were initially generated using 25 cycles and quantified (Qubit 3.0 Flourometer, high sensitivity assay kit). These products were subsequently combined at equimolar concentrations and purified using a Zymo DNA Clean & Concentrator kit (Zymo Research D4014) to create a single library for sequencing. The extraction and PCR steps were repeated for samples that did not attain sufficient DNA concentrations.

DNA libraries were sequenced using an Ion Torrent sequencer (Ion Proton System, Ion Torrent) at the Genomics Core Facility at Saint Louis University with a customized parameter to assess polyclonality after 31bp (the start position of the forward Ion Torrent adapter index sequence). A single sequencing run was used for each pooled library (library 1 – proof-of-concept fitness assays, library 2 – evolution experiment: evolutionary dynamics samples, Generation-0 fitness assays, and Generation-250 fitness assays). An additional library was constructed for a set of samples from library 2 with elevated barcode contamination rates.

Sequence data processing & calculations

Sequence datasets: Sequence data in FASTQ format were parsed and demultiplexed using custom scripts in R (See Code and Data Availability statement, below) A total of 142,243,245 raw reads that matched the forward Ion Torrent adapter indices included in our experiment (omitting reads that matched no forward adapter, polyclonal reads, low quality reads, and adapter dimer reads) were recovered across the three sequenced libraries. 104,365,740 reads (73.4%) were retained for analysis that perfectly matched a forward sequencing adapter index (9-12 bp), reverse sequencing adapter index (9-12 bp) pair, and a MOBY genetic barcode (20 bp) included in the full experimental design.

Barcode contamination rate: The barcoded yeast experimental evolution system has an innate ability to detect and track barcode contamination that could arise during evolution, over the course of short-term fitness assays, or during DNA library preparation. Barcode contamination rate was defined as the mean number of counts mapping to any given barcoded yeast strain

included in the full experimental design (sequenced library), but not expected to be present in the given sample (pair of forward and reverse IonTorrent adapter Indices). Barcode contamination rates were calculated separately for each unique forward-reverse index pair included in each sequencing library and are essentially a measure of how much noise an average contaminating barcode strain contributes to each sample. The barcode contamination rate of sample (primer pair) j, B_j, was measured as,

Equation 1.

$$B_j = \frac{\frac{1}{m}\sum_{i=1}^{m} C_i}{T_j}$$

where *m* is the number of barcoded strains that could potentially contribute to barcode contamination in experiment *j* (i.e., the number of unique strain IDs included in the full library, but not expected in sample j), C_i is the number of barcoded yeast strain counts recovered for contaminating barcode *i*, and T_j is the total number of counts recovered in sample *j* across all barcoded yeast strains included in the full experimental design.

Contamination rate summaries are reported, separately, for the proof-of-concept fitness assays, and the evolution experiment (the latter containing evolutionary dynamics, generation-0 fitness assay and generation-250 fitness assays samples). For the subset of evolution experiment samples that were sequenced in two separate libraries, only the replicate with a lower contamination rate was retained for contamination rate summary reporting and all

275 downstream analyses. In all statistical analyses reported below, contamination rate is initially
276 included as a potential predictor; it is removed via model reduction if deemed nonsignificant.
277
278 **Fitness calculations**: Fitness was evaluated via sequencing-based assays that involved
279 competing barcoded yeast strains against a common ancestral reference strain for 2 days (20
280 generations) at each timepoint in evolution for which fitness metrics were desired. All reported
281 fitness values for the yeast strains in all fitness assays are relative to the same barcoded
282 ancestral reference strain (strain ID: d1H10 for diploids; strain ID: h1H10 for haploids). Briefly,
283 the relative fitness of barcoded yeast strain *i* at generation *gn,* $w_{i\,gn}$, was measured as,
284
285 Equation 2.
286
287 $$w_{i_{gn}} = \left(\left(ln\frac{Ci_{20}}{R_{20}} - ln\frac{Ci_0}{R_0}\right)/20\right)^e$$
288
289 where C*i* and *R* refer to barcode counts for the focal barcode and reference barcode at fitness
290 assay generation 0 (initial mixtures; fitness assay initial measurement) and fitness assay
291 generation 20 (final overnight cultures; fitness assay final measurement), and *20* is the number
292 of generations between measurement at fitness assay generation 0 and fitness assay
293 generation 20 (Hartl and Clark 1997). The change in fitness of strain *i* in the endpoint assays for
294 our 250-generation evolution experiment, Δw_i, we therefore computed as,
295
296 Equation 3.

297 $$\Delta w_i = w_{i_{g250}} - w_{i_{g0}},$$

298

299 where $w_{i\,g0}$ and $w_{i\,g250}$ are the strain's fitness at generation 0 and 250 as measured from

300 Equation 2.

301

302

303 **Statistical analysis**

304 **Analysis & visualization tools:** All Analyses and statistical test were conducted in R version 3.5.2

305 (R Core Team 2012) using the RStudio IDE version 1.1.456 (RStudio Team 2016). Data

306 processing uses almost entirely base-R functionality; the plyr package (Hadley Wickham 2011) is

307 used in some cases for data frame manipulation. All Statistical models with linear mixed effects

308 were generated using the lme4 (Bates et al. 2015), and lmerTest (Kuznetsova, Brockhoff, and

309 Christensen 2017) packages. Weighted t-tests were assessed with the weights package (Pasek

310 2018). Finally, figures and tables were generated with the ggplot2 (Wikham 2009) and sjPlot

311 (Ludecke 2019) packages, respectively; multi-panel figures were built using the gridExtra

312 package (Auguie 2017). Raw p-values are reported unless otherwise noted; the tables included

313 in the supplement report raw and corrected p-values for these instances.

314

315 **Reads:** Analysis of multiplex barcode sequencing data requires careful consideration of sample

316 size. Because counts data are ultimately handled as relative frequencies (proportions), it was

317 necessary to consider underlying sample size or "confidence" in each piece of data within the

318 full dataset for all calculations and analyses. That is, entries with more reads were explicitly

assumed to contribute more to summary calculations and statistical analyses. Variation in sample size was thus controlled for by weighting all calculations by the read sample size and by including such weights in downstream statistical models. This sample size metric considers both the total counts recovered for a multiplexed sample (unique forward and reverse index sequence adapter pair) and the number of counts recovered for the focal barcoded yeast strain(s) for that entry. In the analyses presented here, read calculations utilize harmonic means rather than arithmetic means when data for multiple entries was summarized. Harmonic means were used because they are sensitive to the small values that were typically associated with low focal barcoded strain reads in the dataset.

Proof-of-concept fitness assays: Fitness differences among 92 constructed barcoded yeast strains used for proof-of-concept were assessed using a linear model with mean-corrected fitness as the response variable and yeast strain ID as the predictor variable.

Multiplex barcode sequencing and cross-contamination: Barcode contamination rate was assessed (Equation 2.) and summarized, separately for the proof-of-concept fitness assay and the 250-generation experiment. The effects of barcode contamination rate change in fitness were assessed using a linear mixed effects model with barcode cross-contamination rate as the predictor variable and change in fitness as the response variable. Strain identifier (evolutionary treatment plus yeast strain barcode ID) was included as a random effect nested within evolutionary treatment and was applied only to the intercepts for these models. Additionally, a weighted 1-tailed t-test was utilized to assess whether barcode cross-contamination rates for

341 samples collected in either the fitness assay or the evolution experiment decreased after re-
342 extracting DNA and resequencing.
343
344 **Fitness change in 250 generations of experimental evolution:** Barcoded yeast strains that
345 exhibited increases in fitness over the 250-generation fitness experiment were identified using
346 a linear model with change in fitness as the response variable and a strain identifier (treatment
347 plus yeast strain Barcode ID) as the predictor variable.
348
349 The effects of evolutionary treatment (medium type, ploidy, and transfer dilution) on change in
350 fitness over 250 generations of experimental evolution were assessed using a linear mixed
351 effects model with change in fitness (Δw) as the response variable, and treatment and barcode
352 cross-contamination rate as predictor variables. Additionally, a random effect of a strain
353 identifier (treatment plus yeast strain Barcode ID) was placed on the model intercept.
354
355 **Evolutionary dynamics:** For all analyses of evolutionary dynamics, only the first barcoded yeast
356 strain from each well (sympatric pair) was included to ensure that data were not 'double-
357 counted'. Linear models, with treatment as the predictor variable and either (1) t-max, (2) m-
358 max, (3) t-max-rate, (4) m-max-rate, (5) t-max-diff, (6) m-max-diff, or (7) total cumulative
359 change in barcoded relative abundance across all time-points as the dependent variable were
360 employed to assess treatment differences in evolutionary dynamics. Full models also included
361 initial barcode abundance as a predictor term (in addition to contamination rate) because initial
362 barcode abundance could impact subsequent dynamics. Initial barcode abundance was

subsequently removed from models when nonsignificant, resulting in removal from all but one model (t-max-diff). Barcode fixation rate was not assessed statistically due to the small number of fixation events observed (n=7/76 populations).

Code & data availability

Raw sequence data are available from NCBI's Sequence Read Archive (SRA BioProject ID PRJNA555990). Data formatted for analysis, intermediate data frames, as well as the custom R scripts utilized for all data processing, statistical analysis, and figure generation are available from GitHub (github.com/VinceFasanello/MM_Code_Supplement). A readme file is available in the GitHub repository with the instructions necessary to reproduce the analyses and to confirm the results presented in this article. Supplementary figures, tables, and files are described throughout the main text; detailed descriptions of all supplemental files can be found in File S1. Strains are available upon request.

RESULTS

Proof-of-concept fitness assays

We constructed 92 diploid yeast strains, each with a unique 20 bp barcode inserted upstream of the deleted *HO* gene. We conducted Proof-of-Concept fitness assays to measure any fitness differences among these constructed "barcoded" strains, to estimate our power to detect small fitness differences, and to assess our ability to measure fitness using multiplexed barcode sequencing. We measured fitness simultaneously for our pool of 92 barcodes by the change in

barcode abundance relative to a 'reference' strain (barcode ID: d1H10) in 10 replicates over a two-day period of approximately 20 generations, for a total of 920 fitness assays (92 barcodes x 10 replicates).

A few of the barcoded strains showed significant differences in fitness (3/92 at a 5% FDR, 1/92 at a 1% FDR) (Figure 2, Table S4). The root mean squared error (rMSE) among replicated measures of fitness was 0.0176, indicating good power to detect a 2% fitness difference at nominal significance of 0.05 and a 5% fitness difference at a more stringent cutoff of 0.01 with four replicates (Table S5). With these promising results, we proceeded to conduct a more comprehensive test of the utility of barcoded strains in a practical experimental evolution context.

Experimental evolution

To evaluate the strengths of this barcoded-strain system for studies of experimental evolution, we conducted a 25 day, approximately 250 generation, evolution experiment. Our design included 76 populations, each initiated with two sympatric barcodes. Samples spanned six treatments, which varied in yeast strain ploidy, growth medium, and daily transfer dilution (Table S2). To measure any changes in fitness we competed the evolved generation-250 strains and their generation-0 ancestors against a common reference strain over a two-day period of approximately 20 generations. With four replicate fitness assays for each barcode, this amounted to 1,216 fitness assays (2 barcodes * 2 time-points * 76 populations * 4 replicates). We also measured the change in barcode frequency of sympatric barcoded strains within each

evolving population from 532 longitudinal-evolutionary dynamics samples (76 barcoded pairs * 7 timepoints). From these samples we quantified the magnitude and timing of changes in barcode frequency, which should be influenced by changes in the fitness of the evolving, sympatric barcoded strains present within each population.

Multiplex barcode sequencing: We utilized a two-step multiplexed design to obtain high throughput estimates of fitness based on barcode sequencing in our fitness assays. In the first step we leveraged the strain-identifying barcodes by pooling multiple strains together and simultaneously competing them against an ancestral reference strain to estimate relative fitness. In our second multiplexing step we PCR amplified each fitness assay sample with unique forward and reverse indexed sequencing adaptors. This latter step enabled us to assign sequencing reads to the appropriate fitness assay after sequencing many samples in concert as a single library. We constructed one library for each experiment (Library 1 – Proof-of-Concept fitness assays; Library 2 – 250-generation evolution experiment evolutionary dynamics and fitness assays samples).

From 84,776,627 demultiplexed reads, we obtained a median of 2,961 reads per barcode in each sample. However, we also detected cross-contamination, defined as strain barcodes with sample indexes that shouldn't exist in our sequenced libraries. The average rate of cross contamination per sample was low, 0.04%, and consistently present in nearly all of our samples (Figure S1 A, B.). Contamination could occur during culturing of yeast strains, liquid handling during preparation of libraries (Lenski et al. 1991; Van den Bergh et al. 2018), or via index

429 switching during sequencing procedures (Illumina 2017; Sinha et al. 2017; Costello et al. 2018).
430 The low but uniform rate of cross contamination we observe is more consistent with library
431 preparation and sequencing than yeast contamination. Additionally, no growth was observed in
432 culture blanks during any fitness assays nor during the 25-day experimental evolution
433 experiment.
434
435 To test whether the cross-contamination rate depends on liquid handling during library
436 preparation, we reprocessed a subset of samples with high cross contamination rates using
437 identical starting material (multiple sample aliquots were created at the time of sample
438 collection). Cross contamination rates decreased significantly in these reprocessed samples ($t = 22.3$, $df = 65$, $p < 10e\text{-}6$), but a low level of background contamination remained (Original
439
440 Samples: mean = 0.75%; reprocessed samples: mean = 0.05%) (Figure S2).
441
442 In our analyses, the presence of low abundance cross contamination was removed from all
443 samples in which a barcode is not expected to occur. However, this doesn't eliminate
444 contamination in samples where a barcode is expected to occur. In such cases, error in
445 estimates of barcode frequency is highest when a barcode's frequency is low and approaches
446 the cross-contamination rate. Although results did not greatly change using cross-
447 contamination as a covariate, we included cross-contamination rate in our models (when
448 significant) because it was negatively associated with fitness ($P < 10e\text{-}6$) between generation 0
449 and generation 250 in the fitness assays data from the 250-generation experimental evolution
450 (Figure S3; Table S6).

451

452 **End-point fitness assays**: We assessed fitness in the 154 evolved strains (evolution experiment
453 generation-250 strains) as well as their ancestors (evolution experiment generation-0 strains).
454 For each strain and timepoint, fitness was measured in comparison to a common ancestral
455 reference strain via a two-day competition-based fitness assay in the same conditions under
456 which the strain had been evolved.

457

458 Twenty three percent (35/154) of the strains showed significant increases in fitness between
459 generation 0 and generation 250 at a 1% FDR (Figure 3, Table S7). Within this subset, the
460 average fitness increase was 6.80% with a range of 2.75% to 23.5%. Relatively few strains with
461 significant increases in fitness were found in the CM treatment (3/42; 7.14%) and ethanol stress
462 treatment (2/22; 9.09%). A higher proportion of strains exhibited significant increases in fitness
463 in the lower 1:250 dilution treatment (9/22; 40.9%), the salt stress treatment (11/22; 50.0%),
464 and the haploid treatment (10/22; 45.5%). No strains in the 1:4000 dilution treatment (0/22)
465 exhibited increases in fitness. None of strains (0/154) across all of our treatments exhibited a
466 significant overall decrease in fitness in the course of our experiments.

467

468 Next, we evaluated the effect of evolutionary treatment on fitness change. We found
469 significant variation in fitness among treatments ($P < 10e-6$). Relative to our standard culture
470 conditions -- diploids in CM ("no stress") with 1:1000 transfer dilution, we found greater (more
471 positive) fitness change in diploid strains evolved in salt stress ($P < 10e-6$), in haploid strains
472 evolved in standard culture conditions ($p = 1.13e-2$), and in diploid strains evolved with a

473 reduced (1:250) daily transfer dilution (p = 9.49e-4). Relative to the CM ("no stress") diploid
474 treatment (our standard culture conditions), we found less (less positive) fitness change in
475 diploid strains evolved in ethanol stress (p = 3.99e-3). We found no significant effect of a more
476 extreme daily transfer dilution (1:4000) on fitness change (p=0.39). Contamination rate had a
477 significantly negative effect on fitness (P < 10e-6) (Figure 4, Table S8), which is consistent with
478 the idea that cross-contamination can reduce the power to detect fitness differences.
479
480 **Evolutionary dynamics**: In experimental evolution, adaptation can influence the relative
481 abundance of barcodes evolving in sympatry (Kao and Sherlock 2008; Selmecki et al. 2015). We
482 tracked the relative proportions of 76 barcoded-yeast pairs evolving in sympatry at seven
483 timepoints during our 250-generation evolution experiment (days 0, 10, 15, 20, 22, 24, and 25)
484 to examine the evolutionary dynamics generated by adaptation and other processes (e.g.,
485 drift). We collected 8 measurements from these 532 evolutionary dynamics samples (76
486 populations * 7 timepoints): (1) barcode fixation, (2) the time-point and (3) magnitude of the
487 maximum change in relative abundance in comparison to the starting conditions, (4) the time-
488 point and (5) magnitude of the maximum rate of change between adjacent time-points, (6) the
489 time-point and (7) magnitude of the maximum difference in BC proportions, and (8) the total
490 cumulative change in barcoded relative abundance summed across all time-points.
491
492 Out of the seven measures of adaptive dynamics that were amenable to statistical testing, six
493 significantly differed by treatment (Table 1; see supplemental figures S4:S10 and supplemental
494 tables S9:S15 for individual adaptive dynamics plots and results tables). Relative to the CM-

diploid treatment (our standard culture conditions) both the salt and haploid treatments were associated with a larger maximum change in relative abundance in comparison to the start ($p = 5.24e-5$, $p = 5.85e-3$, respectively) and a more extreme maximum difference in BC proportion ($p = 2.77e-4$, $p = 6.01e-6$, respectively). The salt treatment was also associated with an earlier time-point of the maximum change in abundance relative to the start ($p = 0.01$), and the haploid treatment was associated with an earlier maximum rate of change ($p = 1.35e-5$). The total cumulative change in barcode abundance was greater for the 1:4000 dilution treatment than the 1:1000 dilution treatment ($p = 1.77e-3$). Total cumulative change in barcode abundance was significantly less for haploids than diploids ($p = 4.9e-2$), and significantly less in the ethanol stress treatment than in the CM with no stress treatment ($p = 2.98e-2$). Finally, we observed barcodes that approached fixation in eleven percent (9/76) of our sympatric populations. Most near-fixation events were in the sympatric populations from the salt (3/11; 27.3%) and haploid (5/11; 45.5%) treatments, one instance was observed in the CM-diploid treatment and no instances of near-fixation were observed in the ethanol 1:4000 dilution, nor 1:250 dilution treatments.

DISCUSSION

Experimental evolution has proven to be a valuable approach for studying a range of evolutionary questions. In this study we implemented a genetic barcoding system in *S. cerevisiae* to increase the efficiency and throughput of these types of studies. The premise of our system is that barcoding microbial strains allows us to engage in increasingly complex

517 experimental designs by enabling multiplexing of independent samples, which increases the
518 throughput of fitness assays, and by providing a relatively simple means to track barcode
519 lineage dynamics. Accordingly, we have demonstrated our system's potential for detecting
520 fitness differences in six experimental evolution treatments and have shown that while the
521 typically low levels of barcode cross-contamination we observe cannot be completely
522 eliminated, their effects on inference can be minimized through simple statistical procedures.
523 Below we discuss the merits and drawbacks of our system, and its capabilities to increase
524 efficiency and throughput in experimental evolution research.
525
526 One potential caveat of a barcoding system like the one we propose here, is that barcoded
527 strains are not necessarily identical to one another at the beginning of an experiment even if all
528 barcoded variants are produced from a single ancestral clone. Although we found no significant
529 fitness differences among the majority of barcoded strains, we note that we did indeed observe
530 a few strains with significant deviations from the population mean fitness. Given the location of
531 our barcode insertions (i.e., a currently non-functional region of the genome) it is unlikely that
532 the barcodes themselves generated these fitness differences. A perhaps more likely explanation
533 is that these differences arose from mutations that occurred during transformation (Giaever
534 and Nislow 2014) or shortly thereafter. Regardless of the reason, future users of our
535 experimental approach could either remove strains with fitness differences entirely from their
536 analyses or could instead quantify initial fitness differentials and include them as a covariate in
537 downstream analyses or fitness assays. We note that initial fitness differentials may be of
538 interest themselves, given that they can potentially impact evolutionary outcomes (Barrick et

539 al. 2010; Kryazhimskiy et al. 2014; Jerison et al. 2017) and the types of mutations that
540 successfully spread through an experimental population (MacLean, Perron, and Gardner 2010).
541
542 An ideal experimental evolution system must be able to detect changes in fitness with
543 confidence. Studies are typically designed to carefully measure large fitness effects; these
544 studies commonly report significant fitness changes or advantages in the range of 5-25% (De
545 Visser and Rozen 2006; B. S. Hughes, Cullum, and Bennett 2007; Gresham et al. 2008; R. Dhar et
546 al. 2011; Selmecki et al. 2015). (De Visser and Rozen 2006)(B. S. Hughes, Cullum, and Bennett
547 2007)(Gresham et al. 2008)(R. Dhar et al. 2011)(Selmecki et al. 2015)Some studies are able to
548 detect fitness effects of ~2%; these typically rely on a large amount of replication and/or
549 sequencing-based census techniques to detect small effect sizes. We show that our
550 experimental evolution system can detect fitness effects of 2% with high power using a
551 relatively small number of replicates (n = 4). The high-throughput nature of this system makes it
552 amenable for studies in which either expected fitness changes are small or replication is
553 difficult due to complex experimental designs that require assaying fitness in multiple contexts;
554 the system is particularly advantageous when many strains (tens to hundreds) are included in
555 each treatment.
556
557 Another important consideration when designing an experimental evolution system is that it
558 must be fairly robust to contamination. While culture contamination is rare in experimental
559 evolution (Lenski et al. 1991; T. F. Cooper and Lenski 2010), barcode (or cross-), contamination
560 is possible. Our results are consistent with prior work on this topic. Specifically, while we found

561 no evidence of culture contamination in blank cultures, we detected a uniformly low level of
562 barcode contamination in multiplexed fitness assays and evolutionary dynamics samples.
563 Because there was no conspicuous pattern of cross-contamination, we suggest that the
564 observed contamination was likely to be introduced in our system during sample preparation
565 for DNA sequencing. DNA extraction is a likely source of cross-contamination in samples
566 processed in strip-tubes or 96-well plate formats that prioritize throughput. However, we
567 minimized the chance for contamination in the DNA isolation step in our experiments by
568 isolating DNA with individual reaction tubes for each sample. Still, other sources of
569 contamination are possible, these include primer contamination during the index addition via
570 PCR (Lo, Mehal, and Fleming 1988) and index switching during library construction or
571 sequencing (Illumina 2017; Sinha et al. 2017; Costello et al. 2018). The latter possibility seems
572 nevertheless unlikely because all PCR steps were performed separately prior to pooling of
573 libraries.
574
575 The strength and efficiency of our system is further evidenced by its numbers. A barcode
576 system enabled us to evolve a large number of strains (176) for 250 generations across six
577 treatments, and to conduct a total of 532 evolutionary dynamics measurements and 1,216
578 fitness assays related to these manipulations in a relatively short amount of time. Reassuringly,
579 our results are largely consistent with prior work. We find greater fitness increases, i.e., a
580 greater rate of adaptation, in haploids than diploids. This finding agrees with another study that
581 found faster rates of adaptation and larger effective population sizes in haploids relative to
582 diploids (A. C. Gerstein et al. 2011). In a related study, Selmecki et al., (Selmecki et al. 2015)

583 found faster adaptation in tetraploids than diploids, but no difference in rate of adaptation
584 between haploids and diploids, potentially suggesting a trend opposite to ours of increasing
585 adaptive rate with increasing ploidy. However, differences between haploids and diploids must
586 be treated with caution because there is mounting evidence that haploid yeast evolves towards
587 diploidy under experimental evolution conditions (Aleeza C. Gerstein and Otto 2011; R. Dhar et
588 al. 2011; Selmecki et al. 2015). We also find greater fitness increase in complete medium (CM)
589 plus NaCl stress than in CM alone, which was not surprising given what is known about
590 adaptation to NaCl stress in *S. cerevisiae* (Blomberg 1995; R. Dhar et al. 2011; Park, Yang, and
591 Kim 2015; Tekarslan-Sahin, Alkim, and Sezgin 2018). In contrast, we were surprised to detect
592 less fitness increase in CM plus EtOH stress than in CM alone. There are several non-mutually
593 exclusive explanations for this result: It is possible that ethanol did not present a significant
594 stress (selective pressure) to the cells once they had attained physiological adaptation to the
595 medium, i.e., acclimation (Huang et al. 2018). It is also possible that adaptations to CM and
596 adaptations to ethanol exhibit antagonistic pleiotropy, similar to what has been found in
597 experiments contrasting rich and poor media (Minty et al. 2011) or exploring adaptation to
598 other chemical stressors (Reyes, Abdelaal, and Kao 2013). Pleiotropy could also shed light on
599 the marked adaptation observed in the NaCl treatment given that adaptation to CM and NaCl
600 stress may exhibit complementarity via synergistic or positive pleiotropy (Ostman, Hintze, and
601 Adami 2012; Riddhiman Dhar et al. 2013; McGee et al. 2016; K. A. Hughes and Leips 2017).
602 Finally, we find no difference between the 1:1000 and 1:4000 daily dilution treatments, but we
603 find a greater increase in fitness when a 1:250 transfer dilution was used instead of the
604 standard 1:1000 dilution. While this finding is not necessarily expected (Gerrish and Lenski

1998; De Visser et al. 1999; De Visser and Rozen 2006; Kryazhimskiy, Rice, and Desai 2012), it nevertheless supports earlier findings that less extreme bottlenecks may favor the maintenance of adaptive mutants (Wahl, Gerrish, and Saika-Voivod 2002), and is consistent with evidence for greater mean fitness increase in wide vs. narrow bottleneck populations (Schoustra et al. 2009). It is also consistent with earlier observations that large populations are less adaptively constrained than small ones in simple environments (Rozen et al. 2008).

In addition to high-throughput fitness assays, barcoding enabled us to track sympatric barcoded lineages during the course of experimental evolution (Blundell and Levy 2014; Levy et al. 2015; V. S. Cooper 2018). As expected, we found general agreement between the evolutionary dynamics results and endpoint fitness assay results in our six experimental treatments. For example, the haploid and NaCl stress treatments both displayed dynamics consistent with more extreme increases in fitness, including greater change in barcode abundance relative to the starting conditions and a greater maximum difference in sympatric barcode abundance than diploids in CM. Interestingly, haploids also showed signs of earlier adaptation than diploid strains in similar conditions, as evidenced by an earlier generation of maximum rate of change in barcode abundance (Blundell and Levy 2014; Levy et al. 2015; Selmecki et al. 2015) and a lower total change in barcode abundance over 250 generations. Although this latter result seem paradoxical, it is consistent with the observation that haploids adapt earlier than diploid strains (A. C. Gerstein et al. 2011), and is expected if a greater proportion of the total change in barcode abundance of haploids in our experiments happened in the first 100 generations.

627 Despite significant differences in barcode dynamics, there are some limitations to interpreting
628 these results. Because we mostly assessed abundance every 50 generations, it is possible that
629 we missed some of the adaptive dynamics. Furthermore, barcode frequencies over time were
630 not measured in replicate. Finally, changes in barcode abundance may not be related to final
631 fitness. For example, the 1:4000 transfer dilution bottleneck treatment had elevated rates of
632 change in barcode abundance and a high amount of total change in barcode abundance
633 without a concomitant increase in fitness. We therefore suggest that future studies employ a
634 denser and more even longitudinal-evolutionary dynamics sampling scheme, with replication,
635 to maximize the value of this type of lineage tracking data.
636
637 In summary, we conclude that the barcoded yeast system that we describe here greatly
638 increases the throughput of fitness measurements and provides a relatively simple means for
639 lineage tracking, thereby enabling more complex and potentially more useful experimental
640 evolution designs. We observe that although barcode contamination imposes some limitations
641 on the implementation of this system, it is possible to track the origin and rates of such
642 contamination and, therefore, consider its effects on experimental outcomes. Overall, our
643 findings indicate that this system represents a significant step forward toward the design and
644 implementation of high throughput studies in this field.

REFERENCES

Auguie, Baptiste. 2017. “GridExtra: Miscellaneous Finctions for ‘Grid’ Graphics.”

Bailey, Susan F., François Blanquart, Thomas Bataillon, and Rees Kassen. 2017. “What Drives Parallel Evolution?: How Population Size and Mutational Variation Contribute to Repeated Evolution.” *BioEssays* 39 (1): 1–9. https://doi.org/10.1002/bies.201600176.

Bailey, Susan F., Qianyun Guo, and Thomas Bataillon. 2018. “Identifying Drivers of Parallel Evolution: A Regression Model Approach.” *Genome Biology and Evolution* 10 (10): 2801–12. https://doi.org/10.1093/gbe/evy210.

Barrick, Jeffrey E., Mark R. Kauth, Christopher C. Strelioff, and Richard E. Lenski. 2010. “Escherichia Coli RpoB Mutants Have Increased Evolvability in Proportion to Their Fitness Defects.” *Molecular Biology and Evolution* 27 (6): 1338–47. https://doi.org/10.1093/molbev/msq024.

Bates, Douglas, Martin Mächler, Ben Bolker, and Steve Walker. 2015. “Fitting Linear Mixed-Effects Models Using Lme4.” *Journal of Statistical Software* 67 (1). https://doi.org/10.18637/jss.v067.i01.

Bell, Graham, and Andrew Gonzalez. 2011. “Adaptation and Evolutionary Rescue Environmental Deterioration.” *Science* 332 (June): 1327–30. https://doi.org/10.1126/science.1203105.

Bergh, Bram Van den, Toon Swings, Maarten Fauvart, and Jan Michiels. 2018. “Experimental Design, Population Dynamics, and Diversity in Microbial Experimental Evolution.” *Microbiology and Molecular Biology Reviews* 82 (3): e00008-18. https://doi.org/10.1128/mmbr.00008-18.

667 Blomberg, A. 1995. “Global Changes in Protein Synthesis during Adaptation of the Yeast
668 Saccharomyces Cerevisiae to 0.7 M NaCl.” *Journal of Bacteriology* 177 (12): 3563–72.
669 https://doi.org/10.1128/jb.177.12.3563-3572.1995.
670 Blundell, Jamie R., and Sasha F. Levy. 2014. “Beyond Genome Sequencing: Lineage Tracking
671 with Barcodes to Study the Dynamics of Evolution, Infection, and Cancer.” *Genomics* 104
672 (6): 417–30. https://doi.org/10.1016/j.ygeno.2014.09.005.
673 Burke, Molly K., Gianni Liti, and Anthony D. Long. 2014. “Standing Genetic Variation Drives
674 Repeatable Experimental Evolution in Outcrossing Populations of Saccharomyces
675 Cerevisiae.” *Molecular Biology and Evolution* 31 (12): 3228–39.
676 https://doi.org/10.1093/molbev/msu256.
677 Cooper, Tim F, and Richard E Lenski. 2010. “Experimental Evolution with E. Coli in Diverse
678 Resource Environments. I. Fluctuating Environments Promote Divergence of Replicate
679 Populations.” *BMC Evolutionary Biology* 10 (11).
680 Cooper, Vaughn S. 2018. “Experimental Evolution as a High-Throughput Screen for Genetic
681 Adaptations.” *MSphere* 3 (3): 1–7. https://doi.org/10.1128/msphere.00121-18.
682 Costello, Maura, Mark Fleharty, Justin Abreu, Yossi Farjoun, Steven Ferriera, Laurie Holmes,
683 Brian Granger, et al. 2018. “Characterization and Remediation of Sample Index Swaps by
684 Non-Redundant Dual Indexing on Massively Parallel Sequencing Platforms.” *BMC*
685 *Genomics* 19 (1): 1–10. https://doi.org/10.1186/s12864-018-4703-0.
686 Dhar, R., R. Sägesser, C. Weikert, J. Yuan, and A. Wagner. 2011. “Adaptation of Saccharomyces
687 Cerevisiae to Saline Stress through Laboratory Evolution.” *Journal of Evolutionary Biology*
688 24 (5): 1135–53. https://doi.org/10.1111/j.1420-9101.2011.02249.x.

689 Dhar, Riddhiman, Rudolf Sägesser, Christian Weikert, and Andreas Wagner. 2013. “Yeast Adapts
690 to a Changing Stressful Environment by Evolving Cross-Protection and Anticipatory Gene
691 Regulation.” *Molecular Biology and Evolution* 30 (3): 573–88.
692 https://doi.org/10.1093/molbev/mss253.
693 Garland, Theodore, and Michael R. Rose. 2009. *Experimental Evolution Concepts, Methods, and*
694 *Applications of Selection Experiments*. University of California Press.
695 Gerrish, Philip J., and Richard E. Lenski. 1998. “The Fate of Competing Beneficial Mutations in an
696 Asexual Population.” *Genetica* 102 (107): 127–44. https://doi.org/10.1007/978-94-011-
697 5210-5_12.
698 Gerstein, A. C., L. A. Cleathero, M. A. Mandegar, and S. P. Otto. 2011. “Haploids Adapt Faster
699 than Diploids across a Range of Environments.” *Journal of Evolutionary Biology* 24 (3):
700 531–40. https://doi.org/10.1111/j.1420-9101.2010.02188.x.
701 Gerstein, Aleeza C., and Sarah P. Otto. 2011. “Cryptic Fitness Advantage: Diploids Invade
702 Haploid Populations despite Lacking Any Apparent Advantage as Measured by Standard
703 Fitness Assays.” *PLoS ONE* 6 (12). https://doi.org/10.1371/journal.pone.0026599.
704 Giaever, Guri, and Corey Nislow. 2014. “The Yeast Deletion Collection: A Decade of Functional
705 Genomics.” *Genetics* 197 (2): 451–65. https://doi.org/10.1534/genetics.114.161620.
706 Graves, J. L., K. L. Hertweck, M. A. Phillips, M. V. Han, L. G. Cabral, T. T. Barter, L. F. Greer, et al.
707 2017. “Genomics of Parallel Experimental Evolution in Drosophila.” *Molecular Biology and*
708 *Evolution* 34 (4): 831–42. https://doi.org/10.1093/molbev/msw282.
709 Gresham, David, Michael M. Desai, Cheryl M. Tucker, Harry T. Jenq, Dave A. Pai, Alexandra
710 Ward, Christopher G. DeSevo, David Botstein, and Maitreya J. Dunham. 2008. “The

711 Repertoire and Dynamics of Evolutionary Adaptations to Controlled Nutrient-Limited
712 Environments in Yeast." *PLoS Genetics* 4 (12).
713 https://doi.org/10.1371/journal.pgen.1000303.
714 Hadley Wickham. 2011. "The Split-Apply-Combine Strategy for Data Analysis." *Journal of*
715 *Statistical Software* 40 (1): 1–29. https://doi.org/10.1234/2013/999990.
716 Hartl, Daniel L., and Andrew G. Clark. 1997. *Principles of Population Genetics*. Vol. 116.
717 Sunderland, MA: Sinauer associates.
718 Horinouchi, Takaaki, Shingo Suzuki, Takashi Hirasawa, Naoaki Ono, Tetsuya Yomo, Hiroshi
719 Shimizu, and Chikara Furusawa. 2015. "Phenotypic Convergence in Bacterial Adaptive
720 Evolution to Ethanol Stress." *BMC Evolutionary Biology* 15 (1): 1–14.
721 https://doi.org/10.1186/s12862-015-0454-6.
722 Huang, Chih Jen, Mei Yeh Lu, Ya Wen Chang, and Wen Hsiung Li. 2018. "Experimental Evolution
723 of Yeast for High-Temperature Tolerance." *Molecular Biology and Evolution* 35 (8): 1823–
724 39. https://doi.org/10.1093/molbev/msy077.
725 Hughes, Bradley S., Alistair J. Cullum, and Albert F. Bennett. 2007. "Evolutionary Adaptation to
726 Environmental PH in Experimental Lineages of Escherichia Coli." *Evolution* 61 (7): 1725–34.
727 https://doi.org/10.1111/j.1558-5646.2007.00139.x.
728 Hughes, Kimberly A., and Jeff Leips. 2017. "Pleiotropy, Constraint, and Modularity in the
729 Evolution of Life Histories: Insights from Genomic Analyses." *Annals of the New York*
730 *Academy of Sciences* 1389 (1): 76–91. https://doi.org/10.1111/nyas.13256.
731 Huxley, Clare, Eric D. Green, and Ian Dunbam. 1990. "Rapid Assessment of S. Cerevisiae Mating
732 Type by PCR." *Trends in Genetics* 6 (C): 236. https://doi.org/10.1016/0168-9525(90)90190-

H.

Illumina. 2017. “Effects of Index Misassignment on Multiplexing and Downstream Analysis.” *Illumina*, 1–4. https://doi.org/10.1101/125724.

Jerison, Elizabeth R., Sergey Kryazhimskiy, James Kameron Mitchell, Joshua S. Bloom, Leonid Kruglyak, and Michael M. Desai. 2017. “Genetic Variation in Adaptability and Pleiotropy in Budding Yeast.” *ELife* 6. https://doi.org/10.7554/eLife.27167.

Kao, Katy C., and Gavin Sherlock. 2008. “Molecular Characterization of Clonal Interference during Adaptive Evolution in Asexual Populations of Saccharomyces Cerevisiae.” *Nature Genetics* 40 (12): 1499–1504. https://doi.org/10.1038/ng.280.

Kassen, Rees. 2014. *Experimental Evolution and the Nature of Biodiversity*. Greenwood Village, CO USA: Roberts and Company publishers, Inc.

Kohn, Linda M., and James B. Anderson. 2014. “The Underlying Structure of Adaptation under Strong Selection in 12 Experimental Yeast Populations.” *Eukaryotic Cell* 13 (9): 1200–1206. https://doi.org/10.1128/EC.00122-14.

Kryazhimskiy, Sergey, Daniel P. Rice, and Michael M. Desai. 2012. “Population Subdivision and Adaptation in Asexual Populations of Saccharomyces Cerevisiae.” *Evolution* 66 (6): 1931–41. https://doi.org/10.1111/j.1558-5646.2011.01569.x.

Kryazhimskiy, Sergey, Daniel P Rice, Elizabeth R Jerison, and Michael M Desai. 2014. “Global Epistasis Makes Adaptation Predictable Despite Sequence-Level Stochasticity.” *Science* 344 (6191): 1519–22.

Kuznetsova, Alexandra, Per B. Brockhoff, and Rune H. B. Christensen. 2017. “LmerTest Package: Tests in Linear Mixed Effects Models .” *Journal of Statistical Software* 82 (13).

https://doi.org/10.18637/jss.v082.i13.

Lenski, Richard E., Michael R. Rose, Suzanne C. Simpson, and Scott C. Tadler. 1991. “Long-Term Experimental Evolution in Escherichia Coli. I. Adaptation and Divergence During 2,000 Generations.” *The American Naturalist* 138 (6): 1315–41. https://doi.org/10.1086/285289.

Lenski, Richard E, PD Sniegowski, and PJ Gerrish. 1997. “Evolution of High Mutation Rates in Experimental Populations of E. Coli.” *Nature* 387 (June): 703–5.

Levy, Sasha F., Jamie R. Blundell, Sandeep Venkataram, Dmitri A. Petrov, Daniel S. Fisher, and Gavin Sherlock. 2015. “Quantitative Evolutionary Dynamics Using High-Resolution Lineage Tracking.” *Nature* 519 (7542): 181–86. https://doi.org/10.1038/nature14279.

Li, Yuping, Sandeep Venkataram, Atish Agarwala, Barbara Dunn, Dmitri A. Petrov, Gavin Sherlock, and Daniel S. Fisher. 2018. “Hidden Complexity of Yeast Adaptation under Simple Evolutionary Conditions.” *Current Biology* 28 (4): 515-525.e6. https://doi.org/10.1016/j.cub.2018.01.009.

Lo, Y. M.D., W. Z. Mehal, and K. A. Fleming. 1988. “False-Positive Results and the Polymerase Chain Reaction.” *The Lancet* 332 (8612): 679. https://doi.org/10.1016/S0140-6736(88)90487-4.

Loewe, Laurence, Volker Textor, and Siegfried Scherer. 2003. “High Deleterious Genomic Mutation Rate in Stationary Phase of Escherichia Coli.” *Science* 302 (5650): 1558–60. https://doi.org/10.1126/science.1087911.

Low-Décarie, Etienne, Marcus Kolber, Paige Homme, Andrea Lofano, Alex Dumbrell, Andrew Gonzalez, and Graham Bell. 2015. “Community Rescue in Experimental Metacommunities.” *Proceedings of the National Academy of Sciences* 112 (46): 14307–12.

https://doi.org/10.1073/pnas.1513125112.

Ludecke, Daniel. 2019. “SjPlot: Data Visualization for Statistics in Social Science.” https://doi.org/10.5281/zenodo.1308157.

MacLean, R. C., G. G. Perron, and A. Gardner. 2010. “Diminishing Returns from Beneficial Mutations and Pervasive Epistasis Shape the Fitness Landscape for Rifampicin Resistance in Pseudomonas Aeruginosa.” *Genetics* 186 (4): 1345–54. https://doi.org/10.1534/genetics.110.123083.

Magtanong, Leslie, Raymond J Andersen, Justin Porter, Sarah L Barker, Corey Nislow, Charles Boone, Minoru Yoshida, et al. 2009. “A Molecular Barcoded Yeast ORF Library Enables Mode-of-Action Analysis of Bioactive Compounds.” *Nature Biotechnology* 27 (4): 369–77. https://doi.org/10.1038/nbt.1534.

McGee, Lindsey W., Andrew M. Sackman, Anneliese J. Morrison, Jessica Pierce, Jeremy Anisman, and Darin R. Rokyta. 2016. “Synergistic Pleiotropy Overrides the Costs of Complexity in Viral Adaptation.” *Genetics* 202 (1): 285–95. https://doi.org/10.1534/genetics.115.181628.

Minty, Jeremy J., Ann A. Lesnefsky, Fengming Lin, Yu Chen, Ted A. Zaroff, Artur B. Veloso, Bin Xie, et al. 2011. “Evolution Combined with Genomic Study Elucidates Genetic Bases of Isobutanol Tolerance in Escherichia Coli.” *Microbial Cell Factories* 10: 1–38. https://doi.org/10.1186/1475-2859-10-18.

Ostman, Bjorn, Arend Hintze, and Christoph Adami. 2012. “Impact of Epistasis and Pleiotropy on Evolutionary Adaptation.” *Proceedings of the Royal Society B: Biological Sciences* 279 (1727): 247–56. https://doi.org/10.1098/rspb.2011.0870.

799 Park, Won Kun, Ji Won Yang, and Hyun Soo Kim. 2015. “Identification of Novel Genes
800 Responsible for Salt Tolerance by Transposon Mutagenesis in Saccharomyces Cerevisiae.”
801 *Journal of Industrial Microbiology and Biotechnology* 42 (4): 567–75.
802 https://doi.org/10.1007/s10295-015-1584-y.
803 Pasek, Josh. 2018. “Weights: Weighting and Weighted Statistics.”
804 Perfeito, Lília, Lisete Fernandes, Catarina Mota, and Isabel Gordo. 2007. “Adaptive Mutations in
805 Bacteria: High Rate and Small Effects.” *Science* 317 (5839): 813–15.
806 https://doi.org/10.1126/science.1142284.
807 R Core Team. 2012. “R: A Language and Environment for Statistical Computing.” Vienna,
808 Austria. http://www.r-project.org/.
809 Reyes, Luis H., Ali S. Abdelaal, and Katy C. Kao. 2013. “Genetic Determinants for n -Butanol
810 Tolerance in Evolved Escherichia Coli Mutants: Cross Adaptation and Antagonistic
811 Pleiotropy between n -Butanol and Other Stressors.” *Applied and Environmental*
812 *Microbiology* 79 (17): 5313–20. https://doi.org/10.1128/aem.01703-13.
813 Roth, Frederick P, Andrew M Smith, Fiona Kaper, Corey Nislow, Guri Giaever, Michael J
814 Thompson, Mark Chee, Lawrence E Heisler, and Joseph Mellor. 2009. “Quantitative
815 Phenotyping via Deep Barcode Sequencing.” *Genome Research* 19 (10): 1836–42.
816 https://doi.org/10.1101/gr.093955.109.
817 Rozen, Daniel E., Michelle G J L Habets, Andreas Handel, and J. Arjan G M de Visser. 2008.
818 “Heterogeneous Adaptive Trajectories of Small Populations on Complex Fitness
819 Landscapes.” *PLoS ONE* 3 (3): 14–17. https://doi.org/10.1371/journal.pone.0001715.
820 RStudio Team. 2016. “RStudio: Integrated Development Environment for R.” Boston, MA:

RStudio, Inc. http://www.rstudio.com/.

Schoustra, Sijmen E., Thomas Bataillon, Danna R. Gifford, and Rees Kassen. 2009. "The Properties of Adaptive Walks in Evolving Populations of Fungus." *PLoS Biology* 7 (11). https://doi.org/10.1371/journal.pbio.1000250.

Selmecki, Anna M., Yosef E. Maruvka, Phillip A. Richmond, Marie Guillet, Noam Shoresh, Amber L. Sorenson, Subhajyoti De, et al. 2015. "Polyploidy Can Drive Rapid Adaptation in Yeast." *Nature* 519 (7543): 349–51. https://doi.org/10.1038/nature14187.

Sinha, Rahul, Geoff Stanley, Gunsagar Singh GS Gulati, Camille Ezran, Kyle Joseph KJ Travaglini, Eric Wei, CKF Charles Kwok Fai Chan, et al. 2017. "Index Switching Causes 'Spreading-Of-Signal' Among Multiplexed Samples In Illumina HiSeq 4000 DNA Sequencing." *BioRxiv*, 125724. https://doi.org/10.1101/125724.

Sniegowski, Paul D., Peter G. Dombrowski, and Ethan Fingerman. 2002. "Saccharomyces Cerevisiae and Saccharomyces Paradoxus Coexist in a Natural Woodland Site in North America and Display Different Levels of Reproductive Isolation from European Conspecifics." *FEMS Yeast Research* 1 (4): 299–306. https://doi.org/10.1016/S1567-1356(01)00043-5.

Swings, Toon, Bram van Den Bergh, Sander Wuyts, Eline Oeyen, Karin Voordeckers, Kevin J. Verstrepen, Maarten Fauvart, Natalie Verstraeten, and Jan Michiels. 2017. "Adaptive Tuning of Mutation Rates Allows Fast Response to Lethal Stress in Escherichia Coli." *ELife* 6: 1–24. https://doi.org/10.7554/eLife.22939.

Tekarslan-Sahin, Seyma Hande, Ceren Alkim, and Tugba Sezgin. 2018. "Physiological and Transcriptomic Analysis of a Salt-Resistant Saccharomyces Cerevisiae Mutant Obtained by

843 Evolutionary Engineering." *Bosnian Journal of Basic Medical Sciences* 18 (1): 55–65.
844 https://doi.org/10.17305/bjbms.2017.2250.
845 Varigny, H. de. 1892. *Experimental Evolution*. London, United Kingdom: MacMillan and Co.
846 Venkataram, Sandeep, Barbara Dunn, Yuping Li, Atish Agarwala, Jessica Chang, Emily R. Ebel,
847 Kerry Geiler-Samerotte, et al. 2016. "Development of a Comprehensive Genotype-to-
848 Fitness Map of Adaptation-Driving Mutations in Yeast." *Cell* 166 (6): 1585-1596.e22.
849 https://doi.org/10.1016/j.cell.2016.08.002.
850 Visser, J. Arjan G M De, and Daniel E. Rozen. 2006. "Clonal Interference and the Periodic
851 Selection of New Beneficial Mutations in Escherichia Coli." *Genetics* 172 (4): 2093–2100.
852 https://doi.org/10.1534/genetics.105.052373.
853 Visser, J. Arjan G M De, Clifford W. Zeyl, Philip J. Gerrish, Jeffrey L. Blanchard, and Richard E.
854 Lenski. 1999. "Diminishing Returns from Mutation Supply Rate in Asexual Populations."
855 *Science* 283 (5400): 404–6. https://doi.org/10.1126/science.283.5400.404.
856 Wahl, Lindi M., Philip J. Gerrish, and Ivan Saika-Voivod. 2002. "Evaluating the Impact of
857 Population Bottlenecks in Experimental Evolution." *Genetics* 162 (2): 961–71.
858 Wikham, Hadley. 2009. *Ggplot2: Elegant Graphics for Data Analysis*. 1st ed. New York: Springer-
859 Verlag New York. https://doi.org/10.1007/978-0-387-98141-3.
860 Zhou, Aifen, Edward Baidoo, Zhili He, Aindrila Mukhopadhyay, Jason K. Baumohl, Peter Benke,
861 Marcin P. Joachimiak, et al. 2013. "Characterization of NaCl Tolerance in Desulfovibrio
862 Vulgaris Hildenborough through Experimental Evolution." *ISME Journal* 7 (9): 1790–1802.
863 https://doi.org/10.1038/ismej.2013.60.
864

AUTHORS CONTRIBUTIONS

J.C.F., C.A.B., P.L., and V.J.F conceived of and designed the study. P.L., and V.J.F. conducted the lab work. V.J.F. processed the data, performed the statistical analysis., and created visualizations. V.J.F., J.C.F., and C.A.B. drafted and edited the manuscript.

COMPETING INTERESTS

The authors have no competing interests.

FUNDING

V.F. was supported by funding provided by the National Science Foundation Graduate Research Fellowship Program (NSF-GRFP) (DGE-1745038) and the Botero and Fay labs. J.C.F. was supported by the National Institutes of Health (GM080669).

ACKNOWLEDGEMENTS

The authors thank the members of the Botero and Fay labs, specifically Angela Chira, Trevor Fristoe, and Emery Longan for ongoing feedback and helpful advice.

885 FIGURES

886

887

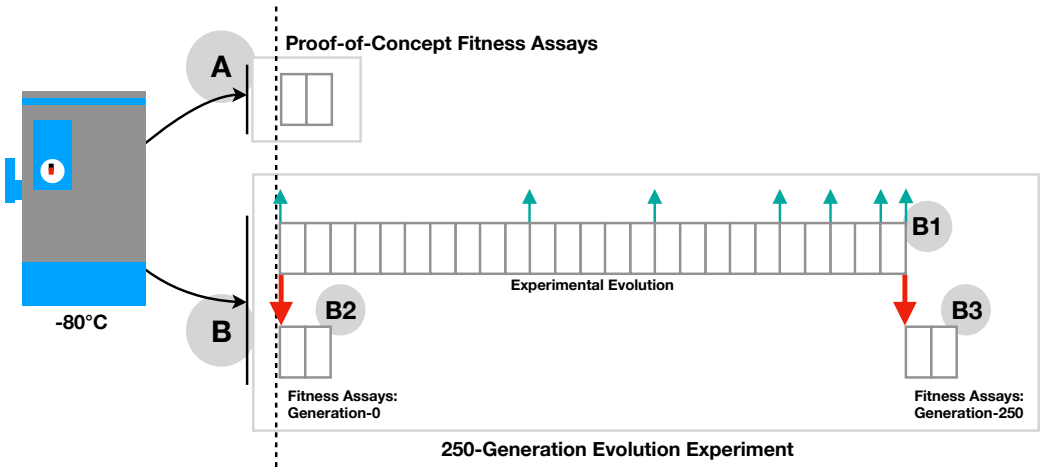

888

889 **Figure 1**

890 Overview of experimental design. Barcoded yeast strains were used for proof-of-concept fitness

891 assays (A, 2 days) and experimental evolution (B, 25 days) with gray boxes indicating one day

892 (10 generations). During the 25-day, 250-generation, experimental evolution (B1), evolutionary

893 dynamics samples were collected at generations 0, 100, 150, 200, 220, 240, and 250 (cyan

894 arrows). Fitness of the ancestral (B2) and evolved (B3) strains were quantified via (2-day, 20-

895 generation) fitness assays (red arrows).

896

897

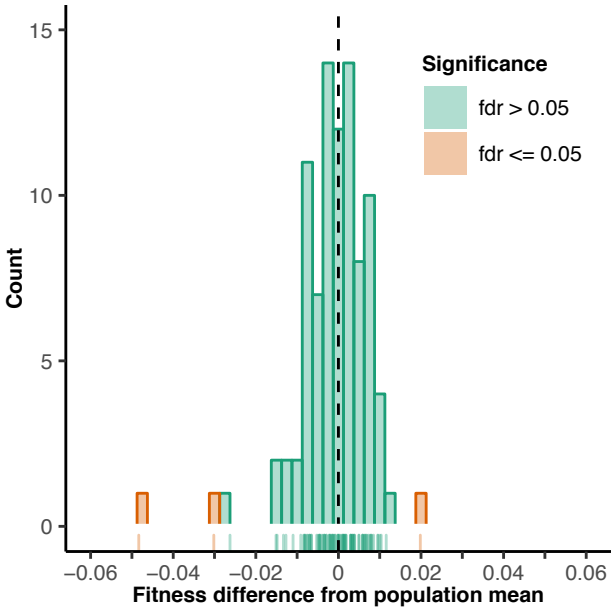

898

899 **Figure 2**

900 Histogram of fitness from 92 barcoded yeast strains. Fitness is the deviation from the

901 population mean and was quantified by competition against a common reference strain via

902 Proof-of-concept fitness assay. Orange and cyan bars indicate yeast strains with fitness values

903 significantly and not significantly different from the population mean at a false discovery rate of

904 5%, respectively.

905

906

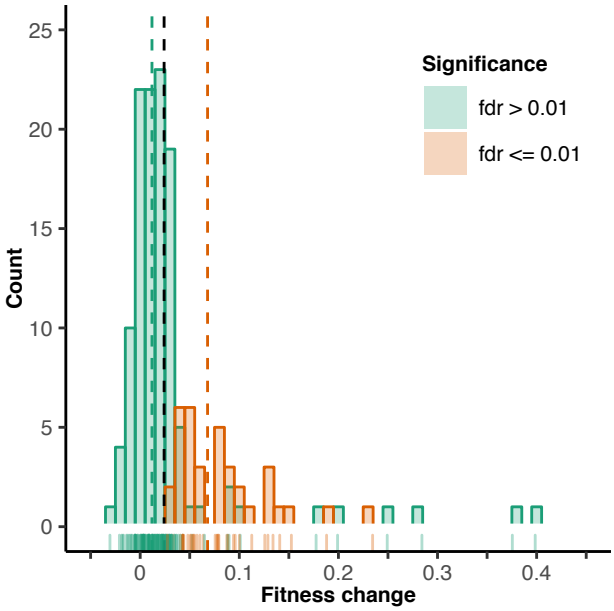

907

908 **Figure 3**

909 Change in fitness over 250 generations of experimental evolution. Histogram depicts fitness

910 increase quantified by competition against a common reference strain. Fitness increase is

911 generation-250 fitness minus generation-0 fitness. Orange and cyan bars indicate strains with

912 fitness values significantly greater or not significantly greater than their own fitness at

913 generation 0 at a false discovery rate of 1%, respectively. No strains significantly decreased in

914 fitness.

915

916

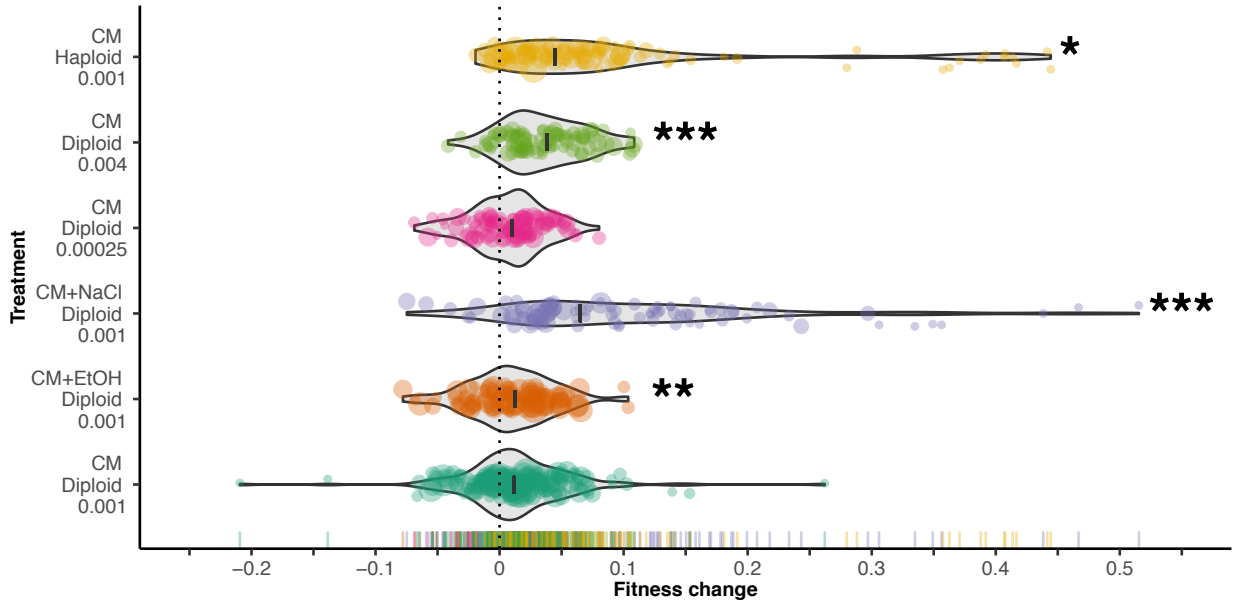

Figure 4

Change in fitness across six treatments in 250 generations of experimental evolution. Violin plots show the density of 152 yeast strains' change in fitness with treatment labels indicating the medium, ploidy and dilution rate. Points indicate individual barcodes with sizes reflecting the number of reads underlying each datapoint and colors indicate evolutionary treatments. Treatment mean fitness changes are depicted as heavy black crossbars. Treatments significantly different from the control treatment are marked with an asterisk. The treatment with diploid yeast evolved under a standard 1:1000 transfer dilution in CM is the reference level in this model.

	Treatment				
	CM + ETOH	**CM + NaCl**	**1:4000 dil.**	**1:250 dil.**	**Haploid**
t-max	N.S.	-48.702 **	N.S.	N.S.	N.S.
m-max	N.S.	0.292 ***	N.S.	N.S.	0.178 **
t-max-rate	N.S.	N.S.	N.S.	N.S.	-52.717 ***
m-max-rate	N.S.	N.S.	0.006 *	N.S.	N.S.
t-max-diff	N.S.	N.S.	N.S.	N.S.	N.S.
m-max-diff	N.S.	0.175 ***	N.S.	N.S.	0.204 ***
total change	-0.007 *	N.S.	0.018 *	N.S.	-0.007 *

Table 1

Associations between evolutionary dynamics and evolutionary treatments. Estimates for significant differences between each evolutionary treatment and the control (CM-diploid, 1:1000 transfer) are shown for seven different measures of barcoded dynamics (t-max, m-max, t-max-rate, m-max-rate, t-max-diff, m-max-diff, and total change).